Reconstructing and Forecasting the Lorenz System

A Study of Embedding, Noise, and Chaos

150751

April 9, 2025

1 Introduction

The Lorenz system is an example of chaotic dynamics, exhibiting high sensitivity on initial conditions and a complicated structure in phase space. My report explores techniques for analysing and reconstructing the Lorenz system, with focus on understanding its predictability. First, the system is modelled and visualised using local dynamical indices to characterise its behaviour. Next, forecasting techniques based on nearest-neighbour methods are implemented to estimate metric entropy. The Lyapunov spectrum is computed to quantify the system's divergence properties. Furthermore, I use time series embedding techniques to reconstruct the system from a single variable, with optimal embedding parameters determined using self-mutual information and Cao's method (Cao, 1997). Finally, the metric entropy is re-evaluated using the embedded time series, and the impact of noise on embedding and entropy is analysed.

2 Methodology

2.1 Modelling and Visualising The Lorenz63 System

The Lorenz63 system is defined by the equations:

$$\frac{dx}{dt} = \sigma(y - x)$$

$$\frac{dy}{dt} = x(\rho - z) - y$$

$$\frac{dz}{dt} = xy - \beta z$$

I solve the Lorenz equations with the standard parameters, $\sigma = 10$, $\rho = 28$, and $\beta = \frac{8}{3}$, and I set the initial conditions as $\mathbf{x}_0 = \mathbf{x}(t = 0) =$

$(1.4324, 2.6837, 18.5043)^T$. I evaluate the trajectory over 50 seconds with 10,000 time-steps. Calculations are only performed on the post-transient phase of the system, defined as between 10 and 50 seconds.

When visualising the Lorenz63 system, local dynamical indices are a useful tool for understanding its complex properties. Local indices capture variations in predictability and structure at different regions of phase space. Three important indices are the local dimension, the extremal index, and the predictability index.

The local dimension (Collet, 2001), denoted d, quantifies the effective number of degrees of freedom near a given point in phase space, providing an estimate of the complexity of the system at that point. A higher local dimension suggests expanding trajectories, indicating greater unpredictability. While a lower local dimension implies that trajectories are more constrained.

The extremal index, denoted θ, characterises the persistence of the trajectory. It provides a measure of how often trajectories cluster when returning to a region in phase space. A value near zero means returns tend to occur in bursts, while a value near one indicates more independent, evenly spaced returns.

The predictability index (Gualandi et al., 2024), α_η, quantifies how long nearby trajectories remain close over a given time lag, providing a measure of local predictability. Higher values of α_η indicate regions in phase space where the system's future evolution is more reliably determined by its current state.

The mathematical formulation for all three local indices is printed in full in (Gualandi et al., 2024).

To estimate the three local indices I implemented a computational approach using python. First, I computed pairwise distances between all states in the Lorenz trajectory using the Euclidean metric. A theiler window was applied to exclude temporally correlated points.[1] The logarithmic returns were then used to identify exceedances beyond the high-threshold quantile, s. Exceedances were extracted and tested for exponentiality to validate their distribution. The mean exceedance associated with the specific reference state was used to calculate local dimension. The extremal index was estimated using the Süveges estimator.[2] The predictability index was estimated by comparing how well neighbours of a point remain close after a time lag.

[1] A trivial addition. Lorenz is deterministic and doesnt have enough randomness to create false neighbours. This is also a noise-free setup (for now). Thereofre, the theiler window is set to zero in my algorithm

[2] The Süveges estimator is a likelihood-based method for estimating the extremal index, it accounts for clustering of extremes in stationary time series data.

2.2 Forecasting and Entropy

Forecasting is the prediction of future states based on the current state of the system. The Lorenz system has sensitive dependence on initial conditions which makes accurate long-term forecasting unreliable. However, short-term forecasting techniques can provide valuable insights. A simple technique is the nearest-neighbour forecasting method, which estimates the future evolution of the system by finding the closest points in the phase space and averaging their future behaviour. The accuracy of these forecasts can be quantified using metric entropy, which measures the unpredictability or randomness of the system's future behaviour based on the current state. By comparing the forecasted values with actual values at different forecasting times, I can assess the system's complexity and understand system entropy. The Pearson's correlation coefficient evaluated across each forecasting time t_{fc} gives solutions for the metric entropy, h, in the equation:

$$ln(1 - r(t_{fc})) = ln(\frac{s_0^2}{2\sigma^2}) + 2ht_{fc}$$

There is a linear relationship between the forecasting time and the natural log of the Pearson correlation coefficient, with a gradient $2h$. [3]

To forecast values in the Lorenz system, I implemented a KDTree nearest-neighbour forecasting algorithm that aims to predict future evolution. The Lorenz dataset was first split into a training set and a test set, each with 50 percent of the total data selected randomly. For a given time, t_{now}, in the test set, I identified the k(=10) nearest-neighbours in the training set. I tracked their evolution over a future time interval, t_{fc}, and averaged their future states to obtain a predicted trajectory. I computed the correlation coefficient between the predicted and true trajectories across each forecasting time, quantifying how well the algorithm captures the system's dynamics. This procedure was repeated for 100 different forecasting times ranging from 0.01 to Lyapunov time , with forecasts performed on 70 randomly selected starting points within the Lorenz system.[4] For each starting time a line of best fit was calculated giving way to 70 entropy predictions, these were averaged to obtain a final entropy prediction. Additionally, Gaussian noise was added to the system with increasingly higher standard deviation values to explore how the entropy evolved with increasing σ values.

2.3 Lyapunov Exponents

Lyapunov exponents measure the sensitivity of a dynamical system to initial conditions by quantifying the average exponential divergence or conver-

[3] It is important to note that this method is primarily used for scenarios where the dynamic rule is unknown, which is not the case for the Lorenz, nonetheless it is still instructive.

[4] Lyapunov time = 1.1 time units

gence of nearby trajectories in phase space.[5] A positive Lyapunov exponent indicates chaotic behaviour, where small perturbations grow exponentially over time, but a negative exponent suggests stable, convergent dynamics. The largest Lyapunov exponent is particularly important since it determines whether a system exhibits chaos. The Lyapunov exponents can be derived by understanding the evolution of the error between an exact trajectory $\mathbf{X}_1$ and a slightly perturbed trajectory $\mathbf{X}_2$:

$$\xi_{12}(t+dt) = A(t)\xi_{12}(t)$$

$$A(t) = I + J_F(\mathbf{X}_1(t))dt$$

Instead of looking at the difference between states we might ask instead, how do the basis vectors evolve? They evolve in the same way, $V_i(t+dt) = A(t)V_i(t)$, however at each evolution they stretch and rotate until eventually they become aligned and no longer span the full tangent space, therefore at each time-step they must be ortho-normalised, $V = QR$. V is the evolved new basis, Q is the ortho-normalised new basis and R is the R-factor matrix, an upper triangular basis containing the coefficients that relate the original basis vectors to the new orthonormal basis. Diagonal elements of R allow for calculation of the Lyapunov Exponents:

$$\lambda_n(t) = \frac{1}{t}\ln|r_{nn}(t)|$$

Where n=1,2,...,n_{max}, and n_{max} = dimension of system.

Furthermore, the Pesin entropy formula establishes a connection between Lyapunov exponents and metric entropy in dynamical systems. The sum of the positive Lyapunov exponents provides an upper bound for the metric entropy of a dynamical system (Pesin, 1977)(Ruelle, 1978) :

$$h \leq \sum_{\lambda_i > 0} \lambda_i$$

2.4 Reconstructing Lorenz Using Embedding

In many real-world scenarios, only partial observations of a dynamical system are available, making it necessary to reconstruct the full phase space from a single measured variable. This process is known as embedding, and it relies on time-delay coordinates to reconstruct the system's attractor in a higher-dimensional space. The fundamental idea, based on Takens' Embedding Theorem (Takens, 1981), states that a scalar time series $x(t)$ can be transformed into an m-dimensional state space by introducing delayed copies of itself, forming a vector $z(t) = (x(t), x(t-\tau), x(t-2\tau), \ldots, x(t-(m-1)\tau))$.

[5]The number of Lyapunov exponents for a system is equal to the number of dimensions of the system.

Essentially, if only the x-component is observed, embedding will allow the recovery of the underlying structure of the system by selecting an appropriate time delay τ and embedding dimension m. Parameter choice is crucial to preserving the topology of the original system and ensuring an accurate reconstruction, so how can we most optimally select τ and m?

To select the best *tau* we use the self-mutual information (SMI), which quantifies the amount of information shared between a time series and its delayed version. It is a measure of the statistical dependence between the present value $x(t_1)$ and the value at a time delay $x(t_1 + \tau)$. [6] For a time series $x(t)$, the SMI at time delay τ is given by the formula:

$$I(x(t), x(t+\tau)) = H(x(t)) + H(x(t+\tau)) - H(x(t), x(t+\tau))$$

Where $H(x(t))$ and $H(x(t+\tau))$ are the entropies of the individual time series, and $H(x(t), x(t+\tau))$ is the joint entropy of the pair of values. The first minimum of the SMI curve corresponds to the optimal time delay τ, where the redundancy between consecutive values is minimised while still retaining enough information to accurately reconstruct the system's phase space. I implement an algorithm that estimates the optimal time delay by computing self-mutual information between a time series and its time-delayed versions for 70 time delays.

Furthermore, to estimate the optimal embedding dimension m, I used Cao's method (Cao, 1997). This involves iteratively embedding the time series $x(t)$ into increasing dimensions $\tilde{m}$ and analysing how the system's phase space evolves. For each embedding dimension $\tilde{m}$, the distance matrix $D_{\tilde{m}}$ is computed, which stores the pairwise distances between points in the embedded space. To prevent the embedding from being overly influenced by points that are too close in time, a theiler window of size w is used to ignore points within w time steps of each other.E_1 measures the scaling of distances as the embedding dimension increases.

$$E_1 = \frac{\langle D_{\tilde{m}} \rangle}{\langle D_{\tilde{m}+1} \rangle}$$

The embedding dimension is optimised when E_1 stabilises near one, indicating that increasing the dimension will no longer significantly change the distances in the phase space, and therefore the dynamics are fully captured.

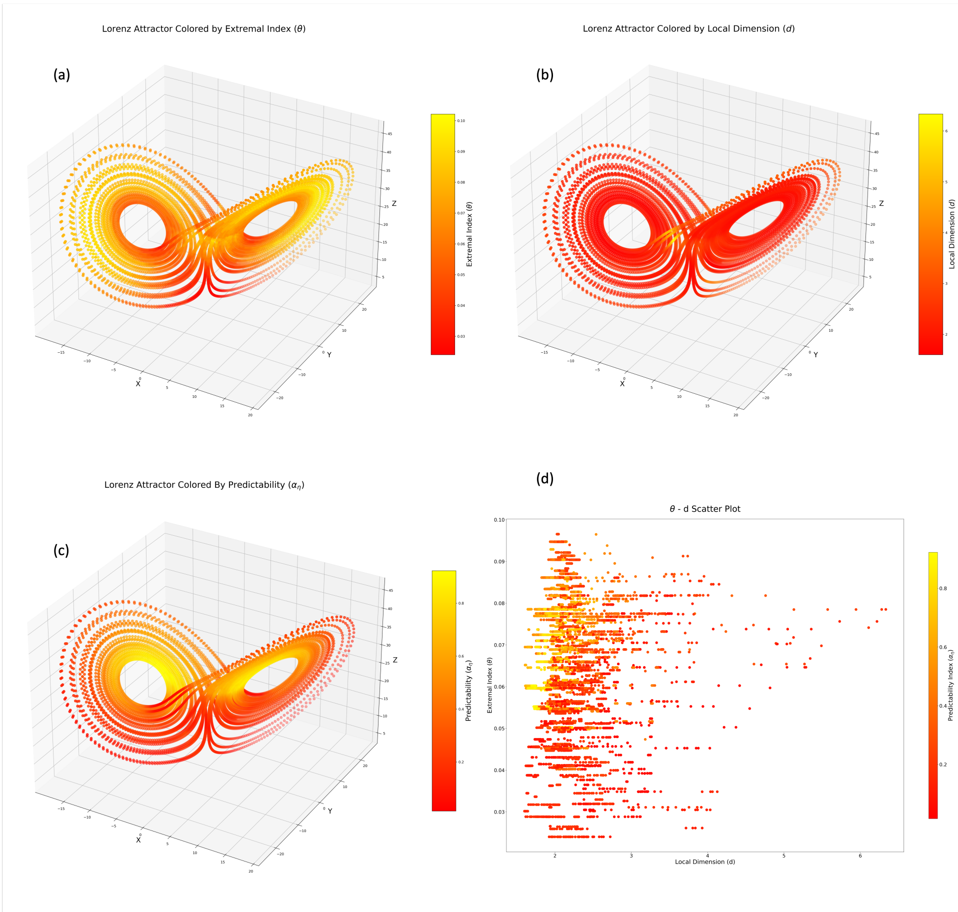

Figure 1: Figure One: Visualisation of the Lorenz attractor coloured by local dynamical indices. The Lorenz attractor is reconstructed over a 50-second integration using 10,000 time-steps, with the first 10 seconds removed to eliminate transients. The attractor is shown three times, each coloured by a different local indicator computed from embedded trajectories: (a) Extremal Index, (b) Local Dimension, (c) Predictability Index, and (d) A scatter plot of θ v d coloured by α_η.

3 Results

3.1 Visualising Local Dynamical Indices

The Lorenz '63 system has a unique butterfly-shaped attractor composed of two lobes that spiral around separate unstable fixed points. Trajectories chaotically move between these lobes, creating a continuous, folded surface in three-dimensional phase space.

From figure 1(a), high θ values occur around the "lobe" regions near periodic orbits. This means the persistence is low in these regions, which is because extreme deviations are less likely to occur consecutively, in other words: extreme events do not cluster together here! This is likely because of longer return times in these outer lobe areas which reduces the likelihood of multiple large deviations occurring in close succession. Additionally, this area is also less sensitive to small perturbations, and this reduced sensitivity means that the trajectory is more predictable. We briefly see high θ values at the intersection of the lobes as well. Each state at the intersection occurs after orbiting round the fixed points, the low frequency of states in this space increases the extremal index. However, these values are bounded by the unpredictability in this area, where trajectories switch orbits, hence θ values aren't as high as on the outer lobes. Low θ regions occur on the inside of the orbits, the trajectories closest to the fixed points. This is because the trajectory gets 'stuck' orbiting the fixed points with high return times, leading to the clustering of events. Trajectories can remain in those regions for extended periods of time before moving to another part of the attractor.

The local dimension of the Lorenz system remains between 2 and 3 for most of the trajectory, with an average value of 2.21, indicating a predominantly low-dimensional chaotic attractor. However, at the midpoint between the two lobes, the local dimension spikes, reaching a value of 6.33. This spike implies a transition to a more complex dynamical state, likely because this is a region of the attractor where trajectories exhibit greater sensitivity to initial conditions.

The predictability index, calculated with a time-lag of 0.2 times the Lyapunov time, shows that the lobes of the attractor initially show high predictability, but this gradually degrades as the trajectories circulate within the lobes. This reduction in predictability suggests that even though trajectories are initially well-defined, their sensitivity to initial conditions increases over time, resulting in a higher uncertainty and a less reliable forecasting.

[6] essentially measures how much knowing one variable reduces uncertainty about the other

3.2 Forecasting and Entropy

To assess the evolution of predictability in the Lorenz-63 system, the predictability index was computed across four forecast horizons: 0.01, 0.05, 0.2, and 1.0 times the Lyapunov time. This is shown in figure 2(a)(b)(d)(e). The results revealed a monotonic decay in mean predictability with increasing forecast time, with corresponding mean values of 0.96, 0.79, 0.40, and 0.074. The big decrease in predictability (from 0.96 at 0.011s to just 0.074 at 1.1s) shows the rapid loss of forecast skill, characteristic of chaotic systems. These results are more clearly shown in figure 2(c) where the PDF of predictability for different forecasting times shows clear trends of poor forecasting at times at or beyond Lyapunov Time.

To quantify this decay more systematically, trajectories were forecasted over 100 evenly spaced forecast times ranging from 0.01 to Lyapunov time according to the algorithm detailed in section 2.2. By fitting a linear model to the logarithmic transformation of $1 - r(t_{fc})$, the metric entropy of the system was estimated to be approximately 0.46, reflecting the exponential growth of forecast errors inherent to chaotic systems. This can be seen in figure 2(f). In section 2.3 Pesin's identity bounds the metric entropy by the sum of the positive Lyapunov exponents. From Figure 3(b), the sum of positive Lyapunov Exponents can be estimated as 1.28, my estimated metric entropy of 0.46 is therefore physically consistent with theoretical expectations for the Lorenz attractor, as it lies below the sum of the system's positive Lyapunov exponents.

Gaussian noise was added to the system with increasingly higher standard deviation values. I evaluated metric entropy over fifty noise values with standard deviations ranging from 0.0001 to 0.1.[7] Theoretically, the entropy of the Lorenz system should increase as more noise is introduced. This is because noise generally introduces more unpredictability into the system, making the system's behaviour harder to predict over time.

Figure 3(a) shows the plot of metric entropy against standard deviation values (σ). The entropy increased linearly from 0.46 to 0.65, indicating that small perturbations in the initial conditions led to a gradual increase in the system's unpredictability. This behaviour aligns with the chaotic nature of the Lorenz system. Beyond σ=0.001, the entropy shows fluctuations, with the magnitude of these fluctuations increasing as the noise level rises. Eventually, noise begins to dominate the deterministic chaotic dynamics which saturates the predictability.

3.3 Lyapunov Exponents

Figure 3(b) shows the Lyapunov Exponents plotted against time for the full 50 second trajectory, the transient time is included in this plot to show the

[7] Trajectory has been scaled with z-score normalisation

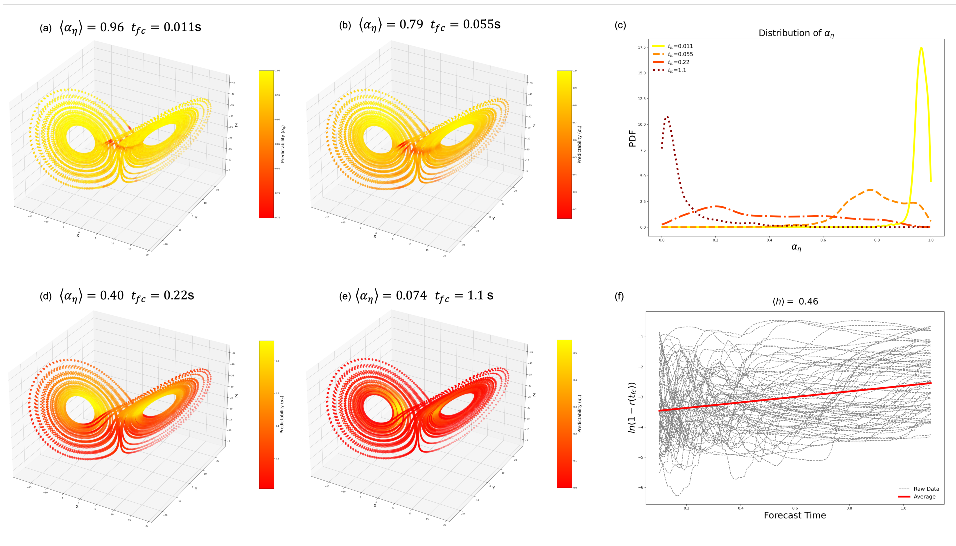

Figure 2: Figure Two. Forecasting and predictability of the Lorenz'63 system over varying forecast times. Plots (a), (b), (d), and (e) display the Lorenz'63 attractor at forecast times of 0.01, 0.05, 0.2, and 1.0 times the Lyapunov time, respectively. The mean predictability indices for these forecast times are 0.96, 0.79, 0.40, and 0.074, showing a progressive decrease in predictability as the forecast horizon increases. Plot (c) shows the probability density function (PDF) of the predictability index for each of the forecast times, illustrating the distribution of predictability across the trajectory. Finally, plot (f) presents the forecast degradation curve, where the metric entropy (h) is estimated based on the decay of the predictability index, capturing the relationship between forecast time and the system's predictability.

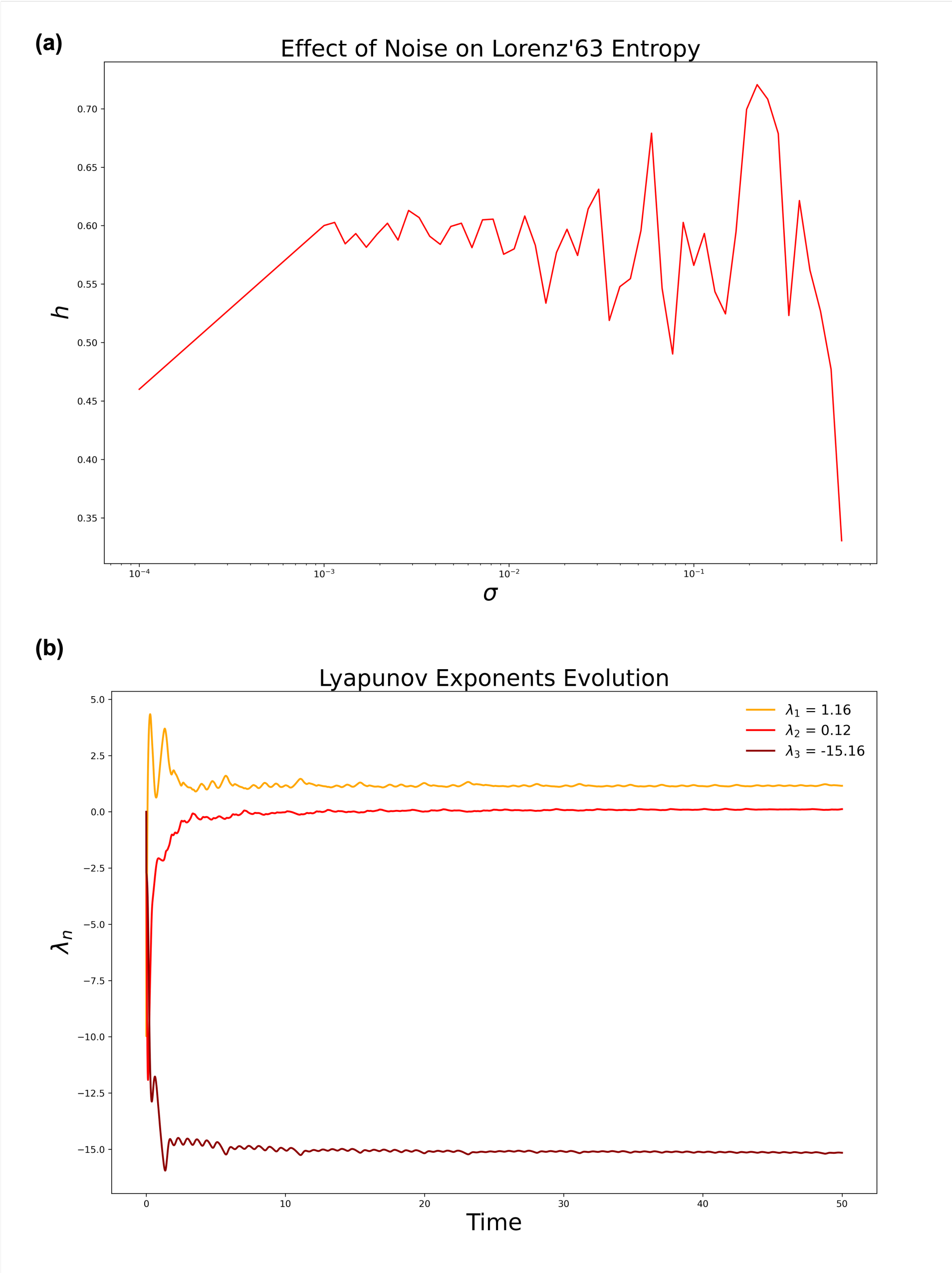

Figure 3: Figure Three. (a) Estimation of entropy for the Lorenz '63 system with varying noise levels. The entropy increases linearly with noise for small standard deviations. Beyond this point, the entropy exhibits fluctuating behaviour, with increasingly larger fluctuations as noise continues to increase. (b) Lyapunov Exponents along the trajectory of lorenz'63. The exponents diverge to a single value which define the system [1.16, 0.12, -15.16]

full divergence to the final Lyapunov values. The Three Lyapunov exponents converge to the finite values [1.16, 0.12, -15.16]. The largest positive exponent ,$\lambda_1 = 1.16$, indicates that the Lorenz system exhibits chaotic behaviour in the x-direction, with nearby trajectories diverging at an exponential rate of approximately 1.16 units per time step. The second Lyapunov exponent, $\lambda_2 = 0.12$, tells me that there is a slower rate of, or zero, divergence along the y direction, suggesting the presence of weak chaos, or transient behaviour. The third Lyapunov exponent, λ_3 = -15.56, suggests that the z direction has strong stability meaning trajectories must be converging rapidly towards each other. These results indicate that while the Lorenz is chaotic in some directions with other regions of stability.

3.4 Reconstructing Lorenz Using Embedding

To determine the best time delay for embedding the Lorenz system, I computed the Self-Mutual Information (SMI) for time delay values up to 70 seconds. As seen in figure 4(a) a minimum SMI value occurs at τ = 32s, meaning it is the optimal delay for embedding the system. Furthermore, the results of the embedding dimension analysis for the Lorenz system indicate the minimum embedding dimension as m=4, which is shown by the convergence of the first normalised mutual information (E_1) values in Figure 4(b). The E1 values start at 0.73 for m=1 and steadily increase until they plateau around 0.97 at m=4, reaching a near-perfect value of 1.0 at higher dimensions. This means that the Lorenz system can be accurately reconstructed with an embedding dimension of 4, which is consistent with theoretical expectations for low-dimensional deterministic systems (Packard et al., 1980). The second normalised mutual information (E_2) values don't converge because the Lorenz system is deterministic and doesn't have randomness to create false neighbours, so the relationships between points stay consistent across dimensions.

Together, these optimal values provide the framework to implement Takens theorem to reconstruct the Lorenz. Figure 4(c) shows the three dimensional plot of the reconstructed Lorenz system.[8] Despite the limitations, the reconstructed attractors shape is fairly similar to that of the Lorenz attractor.

A key metric that has been important throughout my report is the predictability index. The probability distributions of the predictability index at different forecast times reveal differences between the reconstructed Lorenz system and the original, this can be seen in figure 4(d). At short forecast times, both systems exhibit predictability index distributions that are sharply peaked at high values due to strong short-term predictability. How-

[8]This represents a projection of the higher-dimensional phase space onto a three-dimensional subspace, therefore the plot does not capture the full dynamics of the system, as the fourth dimension is omitted

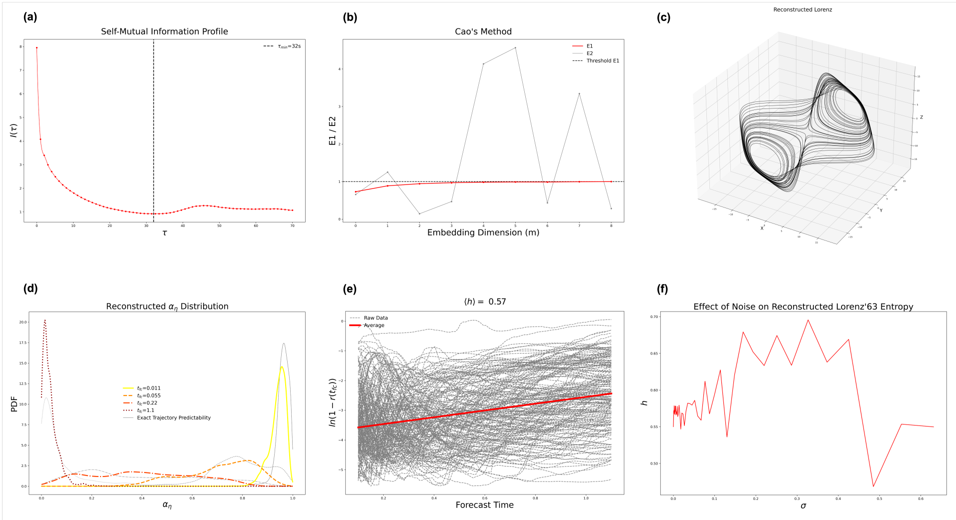

Figure 4: Figure four. (a) Self Mutual Information plotted with increasing embedding times, the minimum indicated optimal embedding time $\tau = 32$. (b) Normalised mutual information with increased embedding dimensions. E_1 plateaus to one at m=4, the optimal embedding dimension is 4. (c) Three dimensional plot of the reconstructed Lorenz system. (d) Reconstructed PDF for predictability index at different forecast times, plotted on-top of the distributions for the exact Lorenz. (e) Metric entropy of the reconstructed four dimensional representation, Its value is higher than the actual Lorenz. (f) Effect of noise on metric entropy

ever, the original Lorenz system produces a narrower and taller peak since it has much better predictability, while the reconstructed system's distribution is slightly broader and lower due to worst predictability. This is also shown at long forecast times, both distributions have low predictability values as expect, but the original Lorenz system displays a broader and lower distribution, again highlighting a better predictability, and the reconstructed system's distribution at these longer times is comparatively more concentrated.

How do entropy calculations performed on the reconstructed Lorenz differ from that performed on the exact Lorenz solution? As seen in figure 4(e), I calculated the metric entropy of the reconstructed four-dimensional Lorenz system as 0.571, based on an ensemble of 200 forecasting trajectories using consistent forecasting times. This value is higher than the metric entropy of the original Lorenz system, which was found to be 0.46. The increased entropy in the reconstructed system further suggests a higher degree of unpredictability in forecasting. Although the reconstruction successfully captures the qualitative structure of the Lorenz attractor, the transformation from a scalar time series to a high-dimensional phase space introduces noise and smoothing effects that lower the precision of trajectory forecasting. As a result, the system is more chaotic than it truly is, highlighting the limitations of phase space reconstruction when recovering the full dynamics.

To investigate the sensitivity of the reconstructed Lorenz system to observational noise, Gaussian noise with standard deviation values logarithmically spaced between 0.0001 and 0.64 and added across 50 levels. At each noise level, the metric entropy was recalculated and the results can be seen in figure 4(f). Initially, the entropy increased gradually from its baseline value by approximately 0.04, before fluctuating slightly and then rising more sharply around $\sigma = 0.05$, reaching values close to 0.7. Beyond this point, the fluctuations became erratic. After $\sigma = 0.5$, the entropy losses any clear trend, indicating that the dynamics were overtaken by stochastic noise. Comparing this graph to figure 3(a), the reconstructed dynamics are more sensitive to noise, likely due to minor reconstruction inaccuracies amplifying uncertainty.

4 Conclusion

The results of this study provide a comprehensive exploration of the Lorenz system's dynamics, predictability, and reconstruction. By visualising local dynamical indices I found that the lobe interiors show low persistence and high predictability, while transitions between lobes highlighted regions of reduced predictability and increased complexity. Forecasting analysis confirmed the inherently chaotic nature of the Lorenz system, with a rapid decay in predictability as forecast time increased. The estimated metric entropy of 0.46 was consistent with theoretical expectations and validated by comparison with Lyapunov exponents. Importantly, entropy increased with the addition of noise, but beyond a threshold, noise dominated and predictability was lost.

I found that the optimal embedding parameters for the Lorenz63 were $\tau = 32$ and $m = 4$, and reconstruction recovered a qualitatively accurate attractor in three dimensions. However, the reconstructed system produced higher metric entropy (0.571) than the true system when forecasting, suggesting a loss in predictability. Probability distributions of the predictability index confirmed this. I also found that the reconstructed dynamics were much more sensitive to noise with much quicker degradation of predictability, especially at intermediate forecast times.

References

Cao, L. (1997). Practical method for determining the minimum embedding dimension of a scalar time series. *Physica D: Nonlinear Phenomena*, 110:43–50.

Collet, P. (2001). Statistics of closest return for some non-uniformly hyperbolic systems. *Ergodic Theory and Dynamical Systems*, 21(2):401–420.

Gualandi, A., Faranda, D., Lucarini, V., Mengaldo, G., and Dong, C. (2024). Revisiting the predictability of dynamical systems: a new local data-driven approach. *arXiv preprint arXiv:2409.14865*.

Packard, N. H., Crutchfield, J. P., Farmer, J. D., and Shaw, R. (1980). Geometry from a time series. *Physical Review Letters*, 45(9):712–716.

Pesin, Y. B. (1977). Characteristic lyapunov exponents and smooth ergodic theory. *Russian Mathematical Surveys*, 32(4):55–114.

Ruelle, D. (1978). An inequality for the entropy of differentiable maps. *Boletim da Sociedade Brasileira de Matemática*, 9(1):83–87.

Takens, F. (1981). *Dynamical Systems and Turbulence*, volume 898, chapter - Detecting strange attractors in turbulence, pages 366–381. Springer, Berlin, Heidelberg.

Appendix A: Code

The full source code used for simulation, analysis, and plotting is available at:

`https://github.com/150751/LorenzProject`